35. C. R. Gwinn, T. A. Herring, I. I. Shapiro, *ibid.*, p. 4755.
36. J. Neuberg, J. Hinderer, W. Zurn, *Geophys. J. R. Astron. Soc.* **91**, 853 (1987).
37. R. D. McPherson *et al.*, *Mon. Weather Rev.* **107**, 1445 (1979).
38. R. D. Rosen and D. A. Salstein, *J. Geophys. Res.* **88**, 5451 (1983).
39. R. Hide *et al.*, *Nature* **286**, 114 (1980).
40. W. Rudloff, *Ann. Meteorol. Neue Folge* **6**, 221 (1973).
41. K. Lambeck and A. Cazenave, *Philos. Trans. R. Soc. London Ser. A* **284**, 495 (1977).
42. K. Lambeck and P. Hopgood, *Geophys. J. R. Astron. Soc.* **71**, 581 (1982).
43. R. B. Langley *et al.*, *Nature* **294**, 730 (1981).
44. W. E. Carter *et al.*, *Science* **224**, 957 (1984).
45. T. M. Eubanks *et al.*, *J. Geophys. Res.* **90**, 5385 (1985).
46. J. O. Dickey, T. M. Eubanks, J. A. Steppe, in (*6*), pp. 137–162.
47. P. J. Morgan, R. W. King, I. I. Shapiro, *J. Geophys. Res.* **90**, 12645 (1985).
48. R. D. Rosen *et al.*, *Mon. Weather Rev.* **115**, 1627 (1987).
49. R. D. Rosen and D. A. Salstein, *J. Geophys. Res.* **90**, 8033 (1985).
50. P. Brosche and J. Sündermann, *Dtsch. Hydrogr. Z.* **38**, 1584 (1985).
51. C. M. Johns, J. O. Dickey, T. M. Eubanks, J. A. Steppe, *Eos* **68**, 1244 (1987).
52. I. Naito and N. Kikuchi, *Geophys. Res. Lett.* **17**, 5 (1990).
53. R. A. Madden, *J. Geophys. Res.* **92**, 8391 (1987).
54. _____, *ibid.* **93**, 5333 (1988).
55. A. J. Miller, *J. Atmos. Sci.* **31**, 720 (1974).
56. G. Branstator, *ibid.* **44**, 2310 (1987).
57. M. Ghil and K. Mo, *ibid.* **48**, 752 (1991).
58. J. D. Anderson and R. D. Rosen, *ibid.* **40**, 1584 (1983).
59. T. M. Krishnamurti and D. Subrahmanyam, *ibid.* **39**, 2088 (1982).
60. T. Yasunari, *J. Meteorol. Soc. Jpn.* **59**, 336 (1981).
61. Zheng Da-Wei, *Chin. Astron. Astrophys.* **3**, 114 (1979).
62. M. Feissel and D. Gambis, *C. R. Acad. Sci. Ser. II* **291**, 271 (1980).
63. M. Feissel and C. Nitschelm, *Ann. Geophys.* **3**, 180 (1985).
64. J. O. Dickey, M. Ghil, S. L. Marcus, *J. Geophys. Res.*, in press; in *The Earth's Rotation and Reference Frames for Geodesy and Geodynamics*, C. Boucher and G. A. Wilkins, Eds. (Springer-Verlag, New York, 1990), pp. 90–97.
65. A. C. Lorenc, *Q. J. R. Meteorol. Soc.* **110**, 427 (1984).
66. K. M. Lau and L. Peng, *J. Atmos. Sci.* **44**, 950 (1987).
67. K.-M. Lau and T. J. Phillips, *ibid.* **43**, 1164 (1986).
68. X. H. Gao and J. L. Stanford, *ibid.* **45**, 1425 (1988).
69. M. Ghil, in *Irreversible Phenomena and Dynamical Systems Analysis in Geosciences*, C. Nicolis and G. Nicolis, Eds. (Reidel, Dordrecht, Holland, 1987), p. 241.
70. _____ and S. Childress, *Topics in Geophysical Fluid Dynamics: Atmospheric Dynamics, Dynamo Theory and Climate Dynamics* (Springer-Verlag, New York/Berlin, 1987).
71. B. Legras and M. Ghil, *J. Atmos. Sci.* **42**, 433 (1985).
72. A. J. Simmons, J. M. Wallace, G. W. Branstator, *ibid.* **40**, 1363 (1983).
73. J. O. Dickey, S. L. Marcus, J. A. Steppe, R. Hide, *Eos* **70**, 1058 (1989).
74. S. L. Marcus *et al.*, in *The Earth's Rotation and Reference Frames for Geodesy and Geodynamics*, C. Boucher and G. A. Wilkins, Eds. (Springer-Verlag, New York 1990); S. L. Marcus, thesis, University of California, Los Angeles (1990).
75. T. M. Eubanks *et al.*, *Trop. Ocean Atmos. Newsl.* **29**, 21 (1985).
76. R. D. Rosen, D. A. Salstein, T. M. Wood, *J. Geophys. Res.* **95**, 265 (1990).
77. M. Stefanick, *ibid.* **87**, 428 (1982).
78. S. G. H. Philander, *El Niño, La Niña and the Southern Oscillation* (Academic Press, New York, 1990).
79. B. F. Chao, *Geophys. Res. Lett.* **11**, 541 (1984).
80. _____, *J. Geophys. Res.* **93**, 7709 (1988).
81. T. M. Eubanks, J. A. Steppe, J. O. Dickey, in (*6*), pp. 163–186.
82. B. F. Chao, *Science* **243**, 923 (1989).
83. J. D. Horel and J. M. Wallace, *Mon. Weather Rev.* **109**, 813 (1981).
84. R. D. Rosen *et al.*, *Science* **225**, 411 (1984).
85. D. A. Salstein and R. D. Rosen, *J. Clim. Appl. Meteorol.* **25**, 1870 (1986).
86. R. Swinbank, *Q. J. R. Meteorol. Soc.* **111**, 977 (1985).
87. W. L. Wolf and R. B. Smith, *J. Atmos. Sci.* **44**, 3656 (1987).
88. G. J. Boer, *J. Geophys. Res.* **95**, 5511 (1990).
89. J. M. Wahr, *J. Atmos. Sci.* **41**, 190 (1984).
90. K. Wyrtki, *J. Geophys. Res.* **89**, 10419 (1984).
91. Y. L. Jia, N. C. Wells, M. A. Rowe, *ibid.* **95**, 5395 (1990).
92. S. G. H. Philander and A. D. Seigel, in *Coupled Ocean-Atmosphere Models*, J. C. J. Nihoul, Ed. (Elsevier, New York, 1990), p. 517.
93. L. V. Morrison, *Geophys. J. R. Astron. Soc.* **58**, 349 (1979).
94. D. D. McCarthy and A. K. Babcock, *Phys. Earth Planet. Inter.* **44**, 281 (1986).
95. L. V. Morrison, *Mon. Not. R. Astron. Soc.* **187**, 41 (1979).
96. R. S. Gross, personal communication.
97. M. J. Bell *et al.*, *Philos. Trans. R. Soc. London Ser. A* **334**, 55 (1991).
98. The authors are grateful to D. L. Anderson, R. W. Clayton, T. M. Eubanks, A. P. Freedman, R. S. Gross, B. H. Hager, S. L. Marcus, R. D. Rosen, D. A. Salstein, M. A. Spieth, J. A. Steppe, C. V. Voorhies, and C. F. Yoder for useful discussions. Helpful comments on the manuscript were made by R. S. Gross and S. L. Marcus, who also assisted with the preparation of some of the diagrams. The work of one of the authors (J.O.D.) is the result of one phase of research carried out at the Jet Propulsion Laboratory, California Institute of Technology, sponsored by the National Aeronautics and Space Administration.

Molecular Recognition at Crystal Interfaces

I. WEISSBUCH, L. ADDADI, M. LAHAV, L. LEISEROWITZ

Nucleation, growth, and dissolution of crystals have been studied by stereochemical approach involving molecular recognition at interfaces. A methodology is described for using "tailor-made" additives designed to interact stereospecifically with crystal surfaces during growth and dissolution. This procedure was instrumental in controlling crystal morphology and in revising the concept of the structure and symmetry of solid solutions. Consequently, it was applied to the transformation of centrosymmetric single crystals into solid solutions with polar arrangement displaying second-harmonic generation and to the performance of asymmetric synthesis of guest molecules inside centrosymmetric host crystals. The method has led to a discovery of a new "relay" mechanism explaining the effect of solvent on crystal growth. Finally, it allowed for the design of auxiliary molecules that act as promoters or inhibitors of crystal nucleation that can be used to resolve enantiomers and crystallize desired polymorphs.

MOLECULAR RECOGNITION AT INTERFACES, SELF-ASSEMBLY, nucleation, and growth, are concepts of central importance in physics, chemistry, and biology. These concepts are manifest in crystals which, in their different functions and forms, are basic components of the world surrounding us, from minerals, ceramics, and microelectronic components, to bone, shells, and teeth.

Growing crystal surfaces can be thought of as being composed of "active sites" that interact stereospecifically with molecules in solution, in a manner similar to the interactions of enzymes and substrates or antibodies and antigens. At the same time, the highly ordered, repetitive arrangements at crystal surfaces, and the knowledge we have of their structures, offer simpler means to pinpoint

Department of Structural Chemistry, The Weizmann Institute of Science, Rehovot 76100, Israel.

molecular interactions. We have used the concept of molecular recognition at interfaces to address a number of open questions in the areas of crystal nucleation and growth, crystal polymorphism, and interactions of the crystal with the growth environment.

Many important studies on crystal growth of a kinetic and thermodynamic nature, some of which take into account molecular interactions, have been reported (*1, 2*). Recently, a stereochemical approach has been adopted that involves growth and dissolution of organic and inorganic crystals in the presence of auxiliaries, which interact with specific crystal faces and may be crystal growth inhibitors or nucleation promoters (*3*). With assistance of molecular auxiliaries, a variety of processes can be performed. Crystals can be engineered with desired morphologies (*4*), a technique which, paradoxically, could reduce the concentration of impurities within the crystal. Preferred crystallization of a desired phase can be induced for the resolution of chiral molecules (*5*) or the precipitation of a polar crystal polymorph (*6*). The absolute structure of chiral molecules or polar crystals can be assigned with the assistance of auxiliaries (7). The symmetry of crystals can be reduced by selective occlusion of the additive, making a "centrosymmetric" crystal display second-harmonic generation (*8*). Molecular crystals can be etched at desired faces on dissolution (*9, 10*), and the influence of solvent on crystal growth may be elucidated (*11*). Designed surfaces, such as Langmuir films, have been used for epitaxially induced crystallization (*12*), and for acquisition of information relevant to the mechanism of the growth of crystals in biological environments.

The key concept for the understanding of all these different processes is molecular recognition at crystal interfaces. We will illustrate this concept with three distinct topics: the reduction in symmetry of crystalline solid solutions, the effect of solvent on crystal growth, and the design of auxiliaries for crystal nucleation.

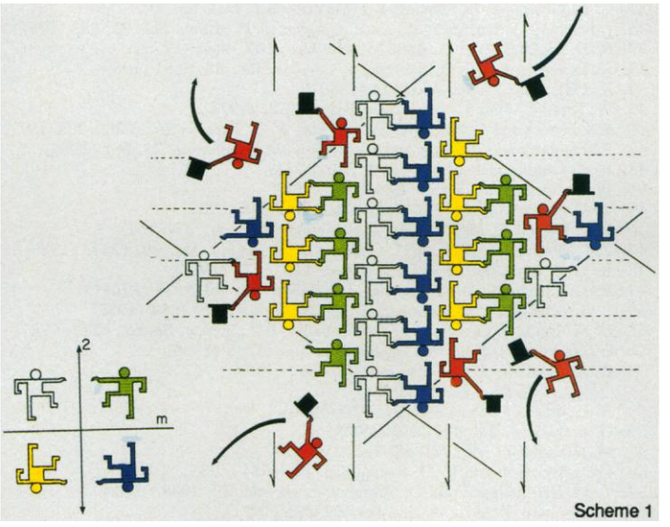

Scheme 1

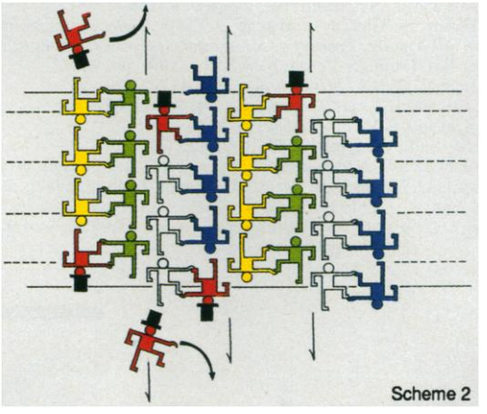
Scheme 2

Reduction in Crystal Symmetry of Solid Solutions

Principles. Crystal surfaces, although determined by the arrangement of the molecules within the crystal lattice, display surface structures that are different from each other and from that of the bulk. In particular, the two-dimensional (2-D) symmetry relating molecules at a certain surface is generally lower than the three-dimensional (3-D) symmetry found within the bulk. For convenience we shall illustrate this aspect through three examples of the same schematic molecular arrangement: the specific point group is $2/m$, which belongs to the space groups most commonly observed in molecular crystals (the symbol $2/m$ specifies a twofold axis 2, perpendicular to a mirror plane m, the combination of which generates a center of inversion $\bar{1}$). This point symmetry (and its subgroups, such as $\bar{1}$, 2, and m), which describes the relative orientations of the molecules in the crystal, is depicted in the key to Scheme 1. In the arrangement shown in Scheme 1, the green men are related to the white men by twofold screw rotation (the axes for which are denoted by half arrows), to the blue men by glide symmetry (the planes for which are denoted by dashed lines), and to the yellow men by centers of inversion. At the four surfaces shown, however, all of these symmetry relations are broken because the faces make an oblique angle with the symmetry axis; thus, their 2-D symmetry is limited to translation, defined crystallographically as $p1$. Scheme 2 describes the same arrangement delineated by a different set of faces, parallel to the glide planes. At these two surfaces, delineated by black lines, the twofold screw symmetry relating the white to the green and the blue to the yellow men is preserved, whereas the glide symmetry (green-blue, yellow-white) and the center of inversion are broken; thus, the faces have symmetry $p2$. Finally, Scheme 3 describes the same structure with still a different set of faces perpendicular to the glide plane. The twofold screw symmetry (white-green, blue-yellow) at the surface is broken, whereas the glide is preserved (white-yellow, green-blue). The 2-D symmetry definition of these faces is pg.

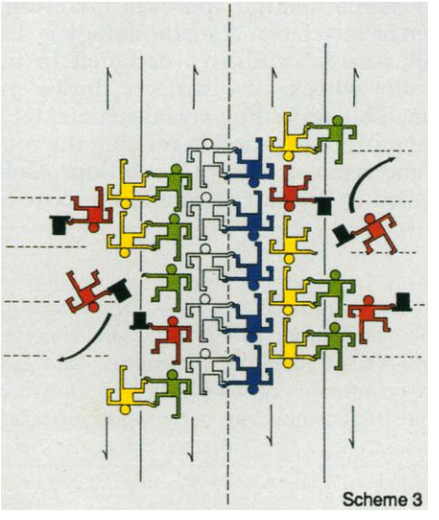
Scheme 3

Note that screw or glide symmetry perpendicular to a surface is not a true symmetry at the surface (although the corresponding rotation and mirror symmetries are true). Nevertheless, the symmetry is preserved in a statistical way with respect to the advancing surface.

Applying this information to the additive molecules in Scheme 2, for example, one can see that an additive molecule (red) bearing an appropriately modified group (hat) can substitute for a substrate molecule at the top surface at the white and the green sites, but not at the yellow and blue sites, because only at the former sites is the regular pattern of interactions at the crystal surface, undisturbed by the modified group. Conversely, at the bottom face, the additive can be adsorbed only at the blue and yellow sites. Thus, the additive molecule would be anisotropically distributed within the grown crystal, preferentially occluded through different subsets of surface sites on the various faces, leading to a mixed crystal composed of sectors coherently intertwined. Occlusion of the additive would thus lead to a reduction of the crystal point symmetry to the symmetry of the surfaces through which it was adsorbed. Thus, in Scheme 1, where the only symmetry element at the given surfaces is translation, the crystal symmetry would be reduced to $P1$. In Scheme 2, where the glide symmetry would be lost after additive adsorption, the crystal symmetry would be reduced to a twofold screw, and, in Scheme 3, to a glide. This principle holds for each crystal sector, although the additive may occupy only a small fraction of all the unit cells. It still holds for the whole crystal, although the different crystal sectors are related to each other by the symmetry elements of the original point group. However, the reduced symmetry of each sector may be masked, depending on the means of detection. For example, the loss of a glide plane or screw axis in a crystal of mosaic texture (that is generally true even for pure organic crystals) would be immediately evident from an x-ray diffraction pattern, but the loss of a rotation axis, mirror plane, or center of inversion would not be.

The adsorption and occlusion of additives may induce a reduction in symmetry, and will, in general, induce a change in the rate of growth of the crystal perpendicular to the adsorbing faces and a concomitant change in morphology, as depicted in Scheme 4.

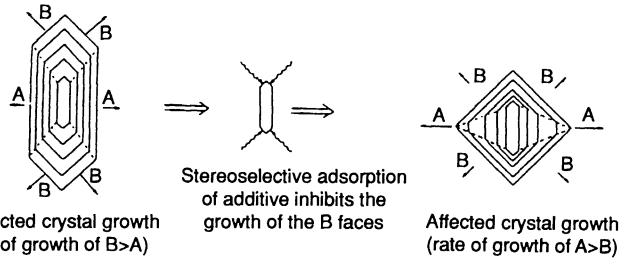

Reduction in crystal symmetry following the above principles was predicted in several host-additive systems and was demonstrated experimentally by a change in crystal morphology, high-performance liquid chromatography, frequency doubling of laser light [that is, second harmonic generation (SHG)], solid-state asymmetric photodimerization, and optical birefringence. It has also been directly observed in other systems by x-ray and neutron diffraction. We now review examples illustrating the arguments described above.

Detection of reduced symmetry by changes in crystal morphology. Glycine, $^{+}H_3NCH_2CO_2^{-}$ is a simple prochiral zwitterionic molecule; that is, the two hydrogen atoms on the central carbon atom are enantiotopic and replacement of one of these hydrogens by a different group yields a chiral molecule. Glycine packs in its crystalline α form (*13*) in an arrangement of point group $2/m$. The faces relevant to the discussion are of the type {010}, as drawn in Scheme

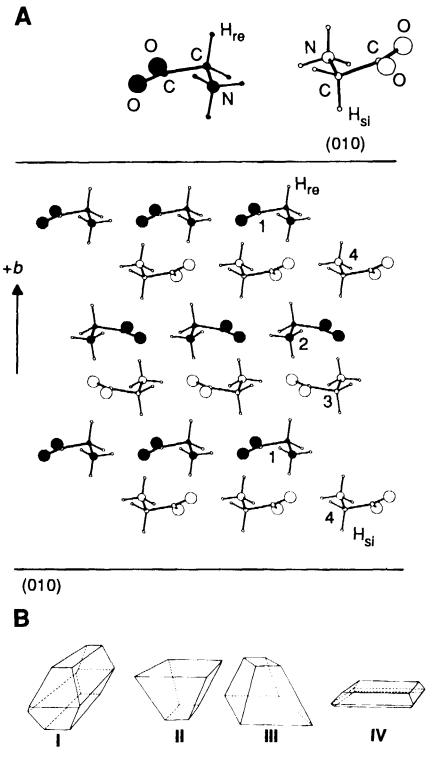

Fig. 1. (**A**) Packing arrangement of α-glycine. Molecules 1 and 2 have their C–H_{re} bonds directed along $+b$; molecules 3 and 4 have their equivalent C–H_{si} bonds along $-b$. (**B**) Crystal morphologies of α-glycine. I is pure α-glycine, and II, III, and IV were grown in the presence of (*R*)-, (*S*)-, and (*R*,*S*)-additives, respectively.

2. Of the four symmetry-related molecules (numbered 1, 2, 3, and 4 in Fig. 1A), 1 and 2, related by twofold screw symmetry, have their C–H_{re} bonds pointing in the $+b$ direction and emerging from the (010) face. By symmetry, molecules 3 and 4, related to 1 and 2 by a center of inversion, have their C–H_{si} bonds pointing toward $-b$ and emerging from the (010) face. Only (*R*)-amino acid additives can substitute for a glycine molecule at the 1 and 2 sites, and then only on face (010), whereas only (*S*)-amino acids can be adsorbed at sites 3 and 4 on face ($0\bar{1}0$). This constraint arises from the steric requirement that the additive molecule be recognized on the {010} surfaces as a "substrate" molecule, with the α-amino acid side chain emerging from the crystal surface. Otherwise, repulsion would occur between the additive and the surrounding molecules on the crystal surface. α-Glycine crystallizes from water as bipyramids (Fig. 1B). (*S*)-amino acid additives induce the formation of pyramids with an ($0\bar{1}0$) basal plane because growth in the $-b$ direction is inhibited. (*R*)-amino acid additives induce the enantiomorphous morphology. Racemic additives cause the formation of {010} plates because growth at the $+b$ and $-b$ sides of the crystal is inhibited. These plates contained 0.02% to 0.2% racemic additive occluded inside the crystal bulk with the two enantiomers totally segregated in the two crystal sectors at the $+b$ and $-b$ halves. As expected, the (*R*)-enantiomers populate the $+b$ half and the (*S*)-enantiomers populate the $-b$ half of the crystal (*14*). In terms of the argument given above, the crystal symmetry of each half of the crystal must be reduced from $P2_1/n$ to $P2_1$, and the two sectors are enantiomorphous. The absolute configuration of the adsorbed amino acid can be directly assigned from the changes in crystal morphology and the enantiomeric distribution of occluded additive.

Detection of reduced symmetry by nonlinear optics. For second-order nonlinear optical effects like SHG (*15*) to be active, the material must be acentric. Thus, SHG is an excellent diagnostic tool for detection of the loss of a crystallographic center of inversion. One requirement is that either the host or additive molecules have large molecular hyperpolarizability tensors β, leading to large optical nonlinearity. Consequently, a centrosymmetric pure crystal struc-

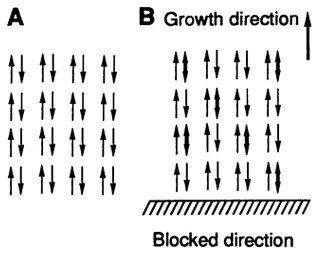

Fig. 2. Schematic illustrating the conversion of (**A**) a centrosymmetric crystal of host molecules with high β coefficients into (**B**) an SHG-active crystal by site-selective occlusion of a centrosymmetric guest molecule.

Fig. 3. The four sectors of platelike crystals of di(11-bromoundecanoyl)-peroxide grown in the presence of the Br. . .CH_3 additive as revealed under crossed polarizers.

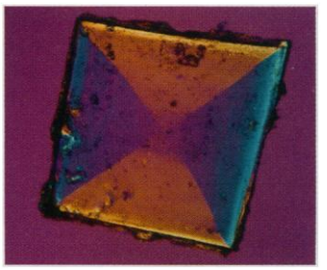

ture, which consists of antiparallel pairs of host molecules with high β coefficients (Fig. 2A), would yield an SHG-active crystal on site-selective occlusion by a centrosymmetric guest molecule (Fig. 2B). Because the growth of the crystal takes place at the top exposed face, the additive is adsorbed and occluded through only one of the pair of surface sites in the growth directions. We demonstrated (*8*) the potential of this approach with centrosymmetric host crystals of *p*-(*N*-dimethylamino)benzylidene-*p'*-nitroaniline, **1a**, which became acentric and SHG-active on site-selective occlusion of the guest molecule *p,p'*-dinitrobenzylideneaniline, **1b**, which is pseudocentrosymmetric. In this system, the host and guest molecules have large and negligible β coefficients, respectively.

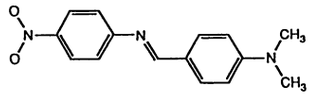

1a

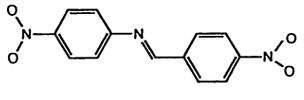

1b

The reverse situation (*8*), where the guest has large hyperpolarizability, is illustrated by α-glycine host crystal containing, as additives, α-amino acids with high β coefficients such as the *p*-nitrophenyl derivatives of α-γ-diaminobutyric acid, **2a**, ornithine, **2b**, and lysine, 2c.

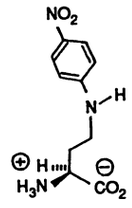

2a

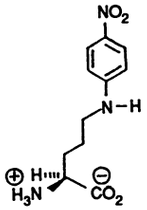

2b

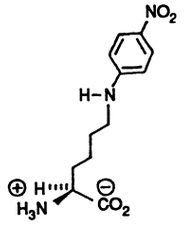

2c

In terms of the arguments presented above, {010} platelike crystals of glycine, grown in the presence of (*R*)- or (*S*)-additives should have symmetry reduced from $P2_1/n$ to $P2_1$. In fact, the symmetry was reduced even further to $P1$, providing additional information on the nature of the crystal growth process (*8*).

Detection of reduced symmetry by optical birefringence. The properties of optical birefringence in crystals have been used to demonstrate a reduction in crystal class. McBride and co-workers (*16*) took advantage of the fact that crystals that belong to a high symmetry class, such as tetragonal, trigonal, or hexagonal, are optically uniaxial, whereas crystals that belong to a lower crystal class, such as triclinic, monoclinic, or orthorhombic, are optically biaxial. They studied the tetragonal crystals of di(11-bromoundecanoyl)peroxide (denoted as Br. . .Br) in the presence of guest where a Br atom is replaced by CH_3 (denoted as Br. . .CH_3). In the host crystal, Br. . .Br molecules assemble into layers that have Br atoms on both the upper and lower surface. Successive layers stack Br to Br atoms with 90° rotation about a fourfold screw axis in the stacking direction. These crystals, which grow as square {001} plates delineated by four {110} side faces, are not birefringent for light traveling along the fourfold screw axis perpendicular to the plate, appearing dark between crossed polarized filters. Crystals of Br. . .Br containing 15% of Br. . .CH_3 are birefringent, the plate revealing four sectors under crossed polarizers (Fig. 3). Birefringence in each sector results from unsymmetrical incorporation of the Br. . .CH_3 additives during crystal growth. As McBride states (*16*), this method of optical microscopy is convenient for surveying large numbers of crystals to catalog their growth patterns and to identify reduced symmetry domains that may be characterized by diffraction.

Probing intermolecular forces through reduced crystal symmetry. There is interest in investigating the minimal modification that would still be recognized and discriminated for by the growing crystal surface and would lead to reduction in symmetry. Solid solutions composed of host and additive molecules of similar structure and shape have been generally believed to exhibit the same symmetries as those of the host crystals.

We first discuss solid solutions of carboxylic acids (XCO_2H) in primary amides ($XCONH_2$), where an OH moiety is substituted for an NH_2 group (Scheme 5).

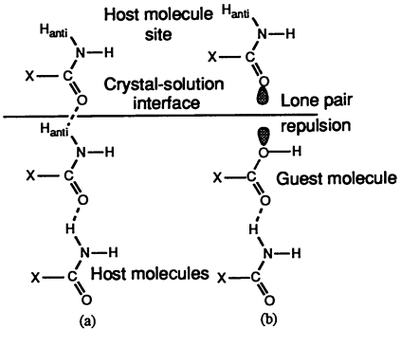

A strong inhibition of growth develops along the direction of the O=C–N–H_a. . .O=C hydrogen bond, where H_a is the amide hydrogen atom in antiperiplanar conformation to the carbonyl. Inhibition arises when a carboxylic acid attempts to force the antiperiplanar lone pair of its OH group against a carbonyl oxygen of the underlying crystal, an atom that would normally form a hydrogen bond with the antiperiplanar hydrogen of the amide. Incorporation of a carboxylic acid in this orientation would substitute a 2 kcal/mol repulsion for a 6 kcal/mol attraction. The carboxylic acid additive molecule would thus avoid surface sites that require the OH group to be oriented toward the surface and would be preferentially adsorbed at sites where the OH group emerges from the surface (*17*).

Reduction in crystal symmetry has been demonstrated in two amide–carboxylic acid systems by neutron diffraction and solid-state

photodimerization. The former technique was applied to asparagine–aspartic acid (*18*), where as much as 15% additive was occluded into the crystal by virtue of the numerous hydrogen bonds between guest and host; the dimerization method was applied to the system *E*-cinnamamide–*E*-cinnamic acid (*19*), where small amounts (<2%) of guest were occluded into the host crystal.

(*S*)-asparagine, $H_2NOCCH_2CH(NH_3^+)CO_2^-$, crystallizes from water as a monohydrate (*20*) with a tight 3-D net of hydrogen bonds in a $P2_12_12_1$ structure (Fig. 4A). The morphology is prismatic, with 18 developed faces (Fig. 4B). Crystallization of (*S*)-asparagine in the presence of (*S*)-aspartic acid, $HO_2CCH_2CH(NH_3^+)CO_2^-$, yields {010} plates (Fig. 4B). In terms of the arguments already given for amide-acid systems, the guest aspartic acid molecule should be more easily adsorbed at sites 1 and 3 on the growing (010) surface than at sites 2 and 4 (Fig. 4C); the reverse situation holds for the opposite ($0\bar{1}0$) face. If, on growth of the mixed crystal, the ($0\bar{1}0$) face is blocked so that the amide and acid molecules would be occluded only through the (010) face, the symmetry of the mixed crystal should be reduced to $P12_11$. A low-temperature (18 K) neutron diffraction study with deuterated aspartic acid in protonated asparagine showed the expected reduction in symmetry (*18, 21*).

Analogously, additive *E*-cinnamic acid induces a loss of the center of inversion in the crystal of *E*-cinnamamide which, in pure form, appears in a centrosymmetric monoclinic arrangement, space group $P2_1/c$. The crystal structure is composed of hydrogen-bonded dimers interlinked by N–H. . .O bonds to form a ribbon-like motif. *E*-cinnamic acid is preferentially occluded through half of the surface sites at the opposite ends of these ribbons, resulting in a crystal with two enantiomorphous halves of $P2_1$ symmetry (Fig. 5), in a manner similar to Scheme 2. This reduced symmetry was proven photochemically (*19*). Ultraviolet irradiation of *E*-cinnamamide yields centrosymmetric photodimers, by virtue of close-packed C=C bonds across centers of inversion (Fig. 5). Replacement of one of such a pair by *E*-cinnamic acid results in formation of asymmetric cinnamamide–cinnamic acid photodimers of opposite chirality at the two enantiomorphous halves of the mixed crystal, with an enantiomeric ratio of 60:40 at each opposite half.

Reduction in crystal symmetry was demonstrated by photodimerization and x-ray and neutron diffraction for the host-guest crystal structure of *E*-cinnamamide–2-*E*-thienylacrylamide (*21*). The host structure incorporates herringbone contacts between aromatic C–H groups and π electron clouds of neighboring phenyl rings. If these contacts are replaced in the host-guest system by unfavorable contacts between sulfur lone-pair electrons and the π electron system, site-selective adsorption and occlusion are induced (Fig. 6A). Thienylacrylamide is occluded through the enantiotopic {011} faces of the crystal (Fig. 6B). These faces exhibit 2-D *p*1 symmetry, as in Scheme 1, because the four different surface sites are not related by symmetry. The guest can easily be adsorbed at only one of these four sites at which the sulfur emerges from the face, leading to *P*1 crystal symmetry. Thienylacrylamide is occluded also through the {001} faces, which exhibit *pg* glide surface symmetry. Adsorption through faces of this type was considered in Scheme 3 and should lead to crystal symmetry *Pc*. The mixed crystal thus should be divided into six sectors of reduced symmetry (Fig. 6C). The different sectors of the same type, such as A and $\bar{A}$, are related to one another by the 2/*m* point symmetry of the host crystal. Low-temperature x-ray and neutron diffraction studies on A- and $\bar{A}$-type sectors, cut from a crystal specimen showed symmetry *P*1, in keeping with the photodimerization studies.

We may draw some general rules for the reduction of crystal symmetry. The local symmetry of a mixed crystal is determined by that of the faces developed. If the symmetry of the crystal face through which an additive is adsorbed is not lower than that of the bulk, there cannot be reduction in symmetry for the crystal sector bound by that face. In other words, the symmetry of a crystal sector cannot be lower than that of the surface of the bounding crystal face. This principle is so basic that, if a crystal is bound by faces of different symmetries, one can, at least in principle, imagine it as formed of different sectors, each with bulk symmetry as low as that of its bounding face, and each sector related to the others by the point symmetry elements of the crystal. Thus, the overall symmetry of the crystal is not reduced. This is a consequence of Curie's

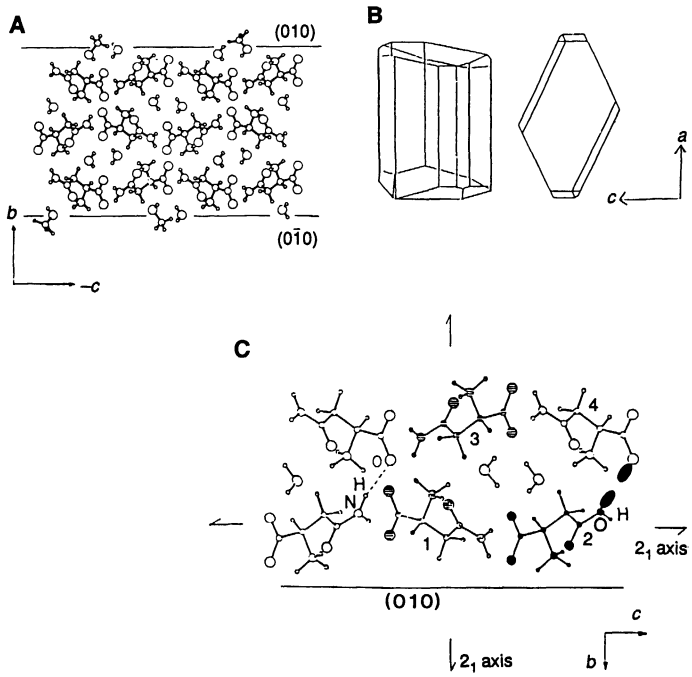

Fig. 4. (**A**) Packing arrangement of (*S*)-asparagine monohydrate viewed along the *a*-axis. The four adsorbed methanol molecules are on the two {010} faces. (**B**) Morphology of (*S*)-asparagine monohydrate. A pure crystal is shown on the left, and a crystal grown in the presence of (*S*)-aspartic acid, or in methanol-water solution is shown on the right. (**C**) Preferential adsorption of aspartic acid on the (010) surface of asparagine (open circles) at sites of type 1 and 3 rather than 2 and 4, as the crystal is growing at the (010) face. Molecules at sites 1 and 3 are shaded, indicating the latter may be occupied by either asparagine or aspartic acid. The probability for aspartic acid to be adsorbed at site 2 (filled circles) is less than at site 1 because of O. . .O repulsion.

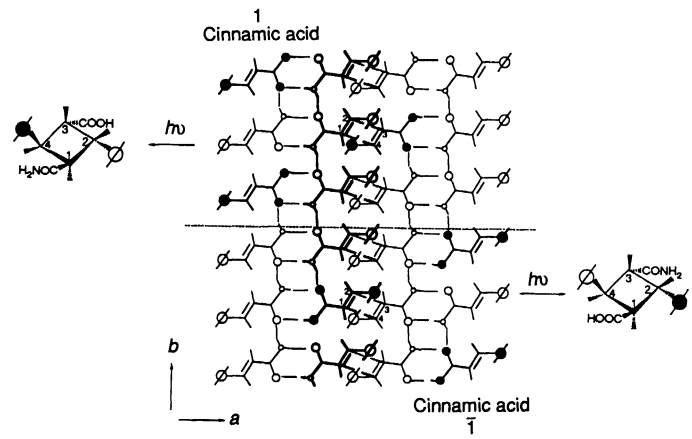

Fig. 5. Ribbon of hydrogen-bonded molecules composed of *E*-cinnamamide (open circles) and occluded guest *E*-cinnamic acid molecules (filled circles). The latter were adsorbed through site 1 at the $+b$ end and site $\bar{1}$ at the $-b$ end.

principle as presented in his paper "Symétrie dans les phenomènes physiques": a physical event cannot have a symmetry lower than that of the event that caused it (*22*). Naturally, no reduction in crystal symmetry may be expected if both host and guest molecules are centrosymmetric, but it is possible if either is. However, if the host molecule has twofold or mirror symmetry (which may be part of the crystallographic symmetry), a reduction is possible even if the guest molecule has the same symmetry.

The Effect of Solvent on Crystal Growth

Analysis of the interactions between crystal surfaces and solvent molecules can be performed following the same rules of molecular recognition applied so far. This treatment provides a different insight into the role of solvent in crystal growth and dissolution. The dilemma is whether strong solvent-surface interactions enhance or inhibit crystal growth. The process of crystal growth from solution can be described in terms of several steps: diffusion of a solute molecule to the surface, stripping of the solute from the solvating molecules, and migration along the surface to a growth site, preferentially a kink site. In general, a rough surface, rich in kinks and steps, would induce faster growth than would a smooth surface. Thus, one accepted theory states that strong solvent-surface interactions, inducing surface roughening, favor fast growth (*23, 24*). On the other hand, one can argue that strong solvent-surface interactions should inhibit crystal growth (*11, 25, 26*), at least in cases in which the rate-determining step for growth is the removal of solvent from the growth site by a solute molecule.

"Tailor-made" solvents. Let us consider first crystals of hydrates, in which water fulfills the task both of solvent and of substrate; when a different solvent, such as methanol, is substituted for water, the new solvent would in a way be similar to an inhibitor molecule. The effect of such tailor-made solvents was examined for two crystals, asparagine·H_2O and rhamnose·H_2O (*27*).

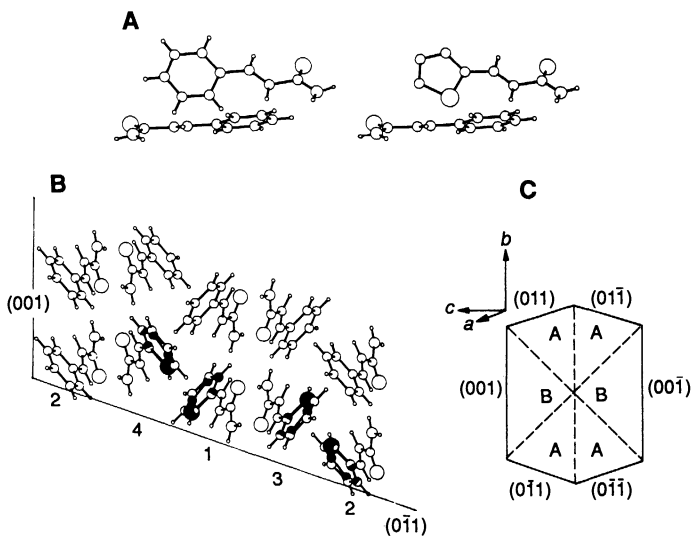

Fig. 6. (**A**) Herringbone contacts involving two cinnamamide molecules (left) or host cinnamamide and guest thienylacrylamide molecules (right). (**B**) The four different surface sites, 1, 2, 3, and 4, of *E*-cinnamamide at the (0$\bar{1}$1) face. Shown shaded are the S and C atoms of the superimposed 2-thienyl rings in the positions they would assume were they to replace cinnamamide molecules at the (0$\bar{1}$1) face. The preferred site for guest adsorption on the (0$\bar{1}$1) face is 1 because the S atom emerges from the crystal face. By the same argument, 1 and 2 are the preferred sites for guest adsorption on the (001) face. (**C**) The morphological representation of cinnamamide-thienylacrylamide crystal with six sectors of reduced symmetry.

In asparagine crystals, the water molecules within the structure (Fig. 4A) are arranged such that one O–H bond emerges from the {010} faces. Gradual substitution of methanol for water causes increasing inhibition of growth at these faces, as expected, if methanol molecules are adsorbed at the site of water molecules, with the methyl group protruding from the face (Fig. 4A). The crystal morphology is gradually modified from prisms into {010} plates, as induced also by aspartic acid (Fig. 4B). The change in morphology of rhamnose monohydrate in the presence of alcohols as cosolvent with water could be explained in an analogous manner.

Fast growth through a "relay" mechanism. A second approach to crystal growth involves selective, strong adsorption of solvent at a subset of molecular surface sites, of type **A**, and repulsion of solvent at the remaining set of surface sites, of type **B**, on the crystal face. This is depicted in Scheme 6, where we emphasize the difference between the two types of sites by assuming a corrugated surface such that the **A**-type site is a cavity and the **B**-type site is on the outside upper surface of the cavity.

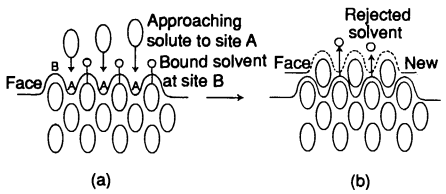

The **B**-type sites are blocked by solvent and the **A**-type sites are unsolvated (Scheme 6a). Thus, solute molecules can easily fit into **A**-type sites. Once the solute molecules are docked into position (Scheme 6b), the roles of the **A**- and **B**-type sites are essentially reversed and the solvent molecules that originally were bound to **B**-type sites would be repelled because they now occupy **A**-type sites. This cyclic process can lead to fast growth by a kind of relay mechanism. This effect may be demonstrated by a crystal with a polar axis; one end exposes the corrugated face and the opposite end a reference face. The experiment then involves a comparison of the relative rates of growth at the opposite poles for the different solvents, as exemplified by the growth and dissolution of the polar crystals of (*R,S*)-alanine and the γ form of glycine in different solvents (*27*).

The two crystals have similar packing features, so the discussion is confined to (*R,S*)-alanine. The molecules are aligned so that the zwitterions expose CO_2^- groups at one end of the polar *c*-axis and NH_3^+ groups at the opposite end. The crystal has a polar morphology (Fig. 7), with the CO_2^- groups emerging at the flat $-c$ end of

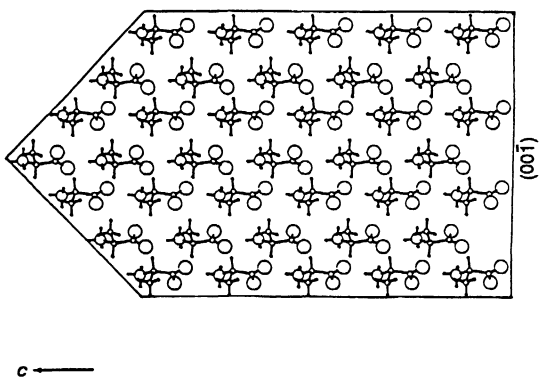

Fig. 7. Packing arrangement of (*R,S*)-alanine delineated by crystal faces, as viewed down the *b*-axis. The capped faces at the $+c$ end of the polar axis expose NH_3^+ and CH_3 groups at their surfaces; the opposite (00$\bar{1}$) faces expose CO_2^- groups.

the crystal and the amino groups at the "capped" $+c$ end. The $(00\bar{1})$ face at the CO_2^- end is corrugated in two perpendicular directions and contains cavities. This face grows and dissolves faster in aqueous solution than the smoother NH_3 faces (*28*). We propose that fast growth at the $(00\bar{1})$ side of the crystal in aqueous solution is due to the relay mechanism of growth (Fig. 8). We predicted that methanol molecules on the other hand, could bind into the cavities at the $(00\bar{1})$ face. The methyl groups of these molecules can form, C–H . . .O(carboxylate) interactions albeit weak, within the cavity and the OH groups can additionally hydrogen-bond to the CO_2^- at the surface. In keeping with prediction, crystals of both (*R,S*)-alanine and γ-glycine grow and dissolve in 70% methanol-water mixtures, preferentially from the NH_3 $+c$ end.

The crystal growth experiments of asparagine monohydrate and rhamnose monohydrate demonstrate than an extension from tailor-made additives to solvents can be made. Namely, the tailor-made solvent can inhibit the growth of the face to which it is strongly adsorbed. We may extend this argument to "normal" solvents that are strongly bound to the surface. However, if the solvent is strongly bound at a subset of sites and repelled (or very weakly adsorbed) at the remaining surface sites (pockets for example), a different set of rules may apply. This case may lead to roughening of the face or, as with γ-glycine and (*R,S*)-alanine, to fast growth by a relay mechanism.

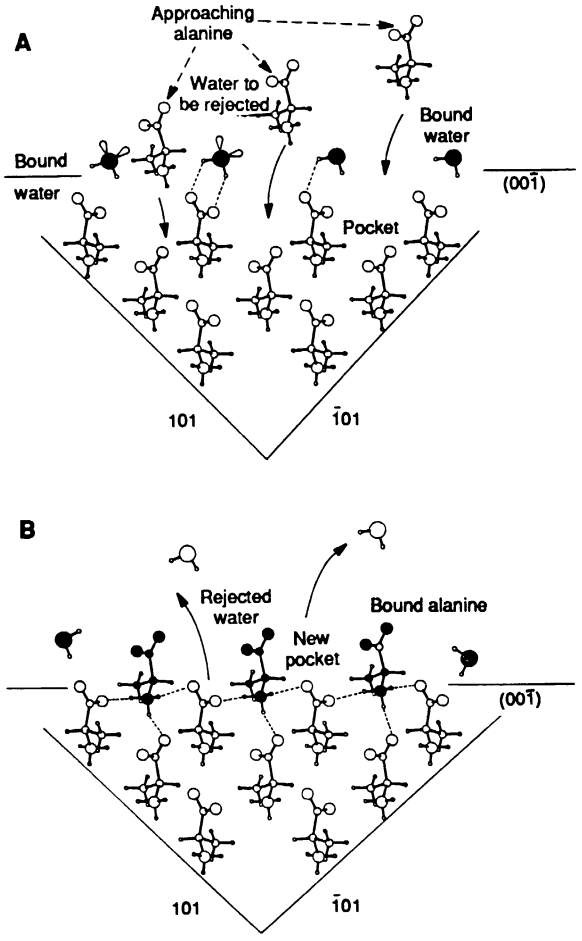

Fig. 8. Schematic representation of the $(00\bar{1})$ face of (*R,S*)-alanine during crystal growth. (**A**) In this view, approaching solute alanine molecules are depicted about to be bound within the pockets of the $(00\bar{1})$ face. Also shown are water molecules bound to the outermost CO_2^- groups of this face. The pockets remain primarily unsolvated because lone pair–lone pair O-O repulsions inhibit the binding of water within them (similar to what has been described in the text for the asparagine–aspartic acid system). (**B**) In this view, the newly adsorbed alanine molecules are each bound by three NH. . .O hydrogen bonds. The previously bound water molecules are shown being rejected by O(water). . .O(carboxylate) lone pair–lone pair repulsions. New unsolvated pockets are formed.

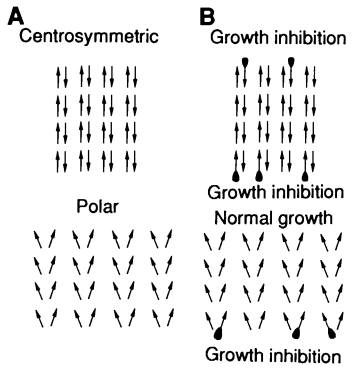

Fig. 9. (**A**) Schematic illustration of the packing arrangement in a polar and a centrosymmetric crystal. The use of an inhibitor in (**B**) blocks growth of the centrosymmetric crystal in two opposite directions but can only inhibit growth in one direction of the polar crystal.

Molecular Recognition in Crystal Nucleation

Design of crystal nucleation inhibitors for control of polymorphism. Formation of crystals from single molecules in supersaturated solutions requires a process whereby these molecules assemble at early stages to form structured aggregates or nuclei. The driving force for the formation of these nuclei is provided by the intermolecular forces within. However, these nuclei develop a surface at the interface with the environment, which is associated with a positive free energy and can destabilize the nuclei. According to classical theory of crystal nucleation, during the growth process nuclei cross a critical radius above which they develop into crystals. A priori, nuclei may assume a variety of structures, some of which are akin to that of the mature crystal. Thus, in systems displaying polymorphism or in systems where there are mixtures of phases, the presence of aggregates of structures resembling each of the various mature phases may be expected. Close to equilibrium conditions, however, only those nuclei corresponding to the thermodynamically stable phase grow into crystals. Following this hypothesis, the structural information stored in the mature crystal may be used for the design of auxiliary molecules that can recognize and interact with the stable crystalline phase and selectively inhibit growth of the nuclei of this phase. If these molecules are designed so that they do not interact with the nuclei of the less stable phase, then this latter phase may precipitate from the solution in a kinetically controlled process, provided the two phases do not display a large stability gap.

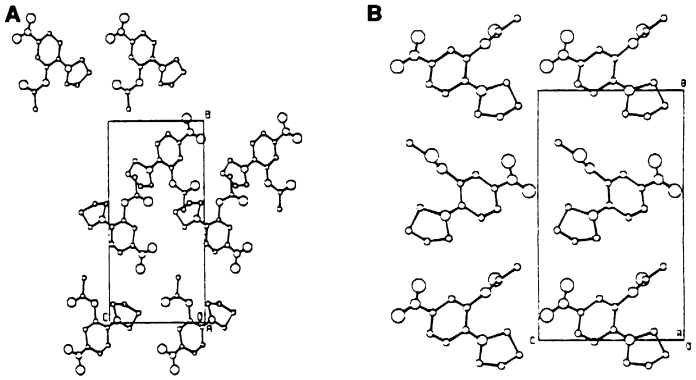

Fig. 10. Packing arrangement of PAN **3** crystal. (**A**) Stable form. The arrangement is pseudocentrosymmetric. (**B**) Metastable form. The polar axis is along *b*.

Conglomerates are a particular case of such a situation in which the two enantiomorphous crystalline phases are equienergetic. Kinetic resolution with the assistance of tailor-made inhibitors was achieved without exception in the systems studied (*5*).

An application in which an energy gap exists is that of racemic histidine·HCl, which precipitates as a stable racemic dihydrate and a metastable conglomerate of resolved monohydrate crystals (*29, 30*). Chiral polymeric inhibitors were designed to inhibit the growth of the stable racemic compound and one of the resolved enantiomorphs. Addition of as little as 1% of the inhibitor induced resolution of the racemic mixture.

Another case involves the preferred precipitation of a polar crystal at the expense of the nonpolar polymorph, also taking advantage of their difference in packing (*6*). In crystals with a polar axis, all of the molecules are aligned in the same direction vis-à-vis the polar axis (Fig. 9A). In nonpolar crystals, whether or not the structure is centrosymmetric, neighboring arrays of molecules along the principal axes are arranged in an antiparallel manner (Fig. 9A). Thus, an appropriate additive would inhibit growth of the nonpolar form at the opposite ends of the crystal (Fig. 9B) but would inhibit growth of the polar form only at one end of the polar axis (Fig. 9B).

A system that satisfies the requirements of the above concept is *N*-(2-acetamido-4-nitrophenyl)pyrrolidene (PAN), **3**, the metastable polar form of which (Fig. 10) displays optical SHG.

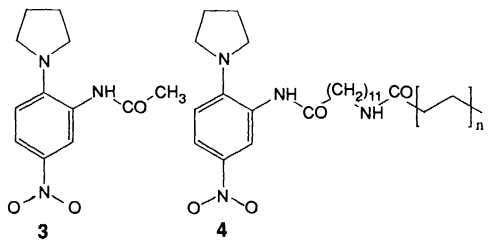

3 **4**

As little as 0.03% of the inhibitor **4** induced crystallization of PAN in its metastable polymorph. In other systems, however, the situation may be more complex; for example, the polar form may belong to a crystal class of high symmetry, such that the host molecules adopt a variety of orientations relative to the polar axis.

Design of crystal nucleation promoters. Nucleation is generally a heterogeneous process. This means that the activation barrier for nucleation is lowered by interaction with foreign surfaces. This process can happen at levels of specificity that range from nonspecific adsorption to oriented growth. One can therefore envisage induced nucleation of crystalline structures with a specific crystal orientation by design of nucleation promoters that match the structure of the crystal on a specific plane, resulting in epitaxial crystallization.

We consider first the induced oriented crystallization (*31*) of α-glycine at the water surface when grown in the presence of minor amounts of hydrophobic α-amino acids, such as valine, leucine, or phenylalanine. These molecules, in pure form, crystallize in hydrogen-bonded layers (Fig. 11, A and B) similar to the layer formed by α-glycine (Fig. 11C). In solution, these molecules tend to concentrate at the water surface with their polar head groups pointing into the water. On the assumption that these molecules form ordered clusters arranged in a manner akin to the layer structure of α-glycine (*32*), they would induce nucleation of α-glycine at the water surface from its (010) or ($0\bar{1}0$) face, the orientation depending on the chirality of the additive. The experimental results were in keeping with this prediction. Moreover, the additives neopentyl glycine and *tert*-butyl glycine did not induce oriented nucleation of glycine because their side groups are too bulky to form a layer as in α-glycine. Thus we concluded that the hydrophobic α-amino acids such as leucine, valine, and phenylalanine form ordered clusters on the water surface that act as epitaxial matrices for oriented nucleation of glycine. However, there is as yet no direct evidence of the extent of crystallinity of these aggregates. To provide further insight into this problem, we carried out the same crystallizations underneath Langmuir monolayers of amphiphilic amino acids with different cross-sectional areas per molecule (*12*). Again, the monolayers that induced oriented nucleation were only those, such as palmitoyl lysine, **5**, that could form 2-D layers similar to the layer formed by α-glycine. The 2-D crystallinity of such monolayers was demonstrated by grazing incidence x-ray diffraction (GIXD) with synchrotron radiation (*33, 34*), which confirmed for **5** a packing arrangement of head groups ($^{+}H_3NCHCO_2^{-}$) similar to that of α-glycine.

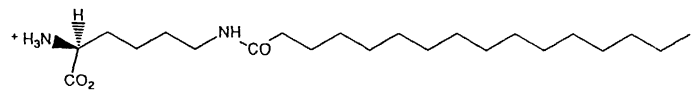

5

The 2-D crystallinity of uncompressed monolayers on the water surface is not a limited phenomenon; it was demonstrated by GIXD in fluorocarbon long-chain α-amino acids at room temperature (*35, 36*), and in hydrocarbon chain alcohols (*37*), amides (*38*), acids (*38*), and acids bound to divalent ions (*39*), at temperatures below ~10°C.

Several crystals other than glycine have been nucleated at the water surface through Langmuir monolayers by virtue of either a structural fit or an electrostatic attraction. These include efficient nucleation of ice under aliphatic alcohols (*37*) and induced crystallization of NaCl (*40*) and of the vaterite and calcite forms of $CaCO_3$ under carboxylic acid monolayers (*41, 42*).

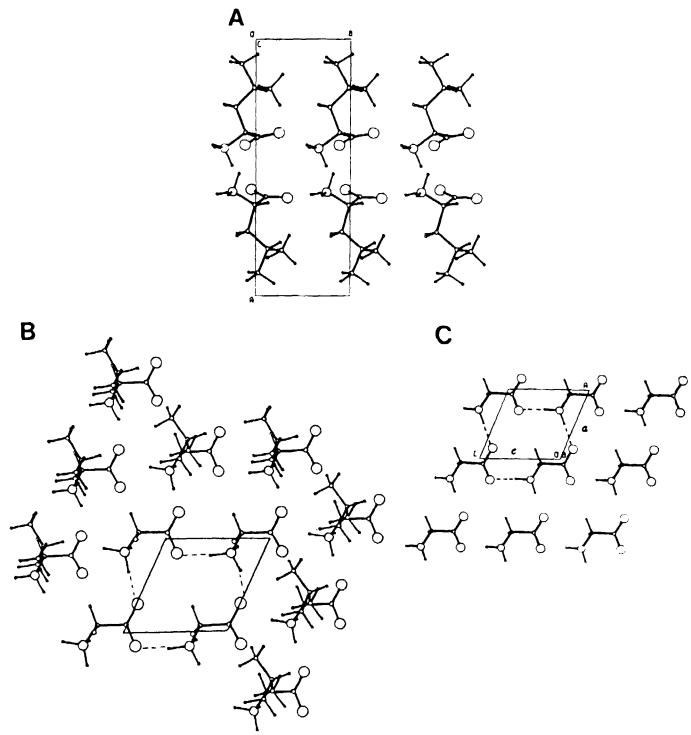

Fig. 11. (**A**) Crystal-packing arrangement of (*S*)-leucine showing hydrogen-bonded bilayers. (**B**) Packing arrangement of (*S*)-leucine viewed perpendicular to the hydrogen-bonded layer. For clarity, the side chains are not drawn for the four molecules forming a cell. (**C**) Layer structure of α-glycine. The structure is similar to the leucine cell in (B).

Conclusions

The role played by molecular recognition at interfaces of 3-D and 2-D crystals has been illustrated. Simple concepts and well-designed molecular interactions can be used in the examination of a variety of problems, for example, control of crystal morphology by design, engineered reduction in crystal symmetry, elucidation of the influence of solvent on crystal growth, exclusive crystallization of a desired polymorph, and induced 3-D crystallization by epitaxy through the design of 2-D crystals. Understanding the solvent effect and controlling crystal polymorphism and crystal shape through molecular additives is of importance in industrial crystallization, particularly for pharmaceuticals. It is well known that crystals of silver iodide have been exploited for promoting rain by induced nucleation of ice in clouds.

Although the focus in this article is primarily on crystal nucleation and growth of organic systems, the approach is also valid for inorganic crystals. It thus has bearing on many facets of materials science involving ordered matrices with special properties, where design and understanding go hand in hand. The technological advances in controlling the microstructure of inorganic materials on the subnanometer scale have led to tremendous success in the preparation of ceramics, synthetic layered microstructures, and semiconducting materials. Paradoxically, advances in the field of organic materials have not been so striking, although the Langmuir-Blodgett technique for the preparation of organic films holds great promise for preparation of pyroelectric and piezoelectric devices and the like. By comparison, in living systems, organisms can mold crystals of specific morphologies, sizes, and orientations in the form of composites of minerals and organic materials with characteristics vastly different from those of their inorganic counterparts (*43*). Indeed, biologically formed minerals have special mechanical and morphological properties by virtue of their intimate contact with the assembly of matrix macromolecules (*44*). The outcome of these selective interactions may be oriented nucleation of ordered crystalline phases or controlled intercalation of protein inside single crystals (*45*). Through an understanding of such processes, it may be possible to prepare synthetic composites with desired properties.

REFERENCES AND NOTES

1. H. E. Buckley, *Crystal Growth* (Wiley, New York, 1951); A. F. Wells, *Philos. Mag.* **37**, 605 (1946).
2. R. Kern, *Bull. Soc. Fr. Mineral. Cristallogr.* 76, 397 (1953); B. M. Smythe, *Austr. J. Chem.* **20**, 1115 (1967).
3. L. Addadi *et al.*, *Angew. Chem.* **24**, 466 (1985).
4. L. Addadi *et al.*, *Nature* **296**, 21 (1982).
5. L. Addadi, S. Weinstein, E. Gati, I. Weissbuch, M. Lahav, *J. Am. Chem. Soc.* **104**, 4610 (1982).
6. E. Staab, L. Addadi, L. Leiserowitz, M. Lahav, *Adv. Mater.* **2**, 40 (1990).
7. L. Addadi, Z. Berkovitch-Yellin, I. Weissbuch, M. Lahav, L. Leiserowitz, *Topics in Stereochemistry* (Wiley, New York, 1986), vol. 16, pp. 1–85.
8. I. Weissbuch, M. Lahav, L. Leiserowitz, G. R. Meredith, H. Vanherzeele, *Chem. Mater.* **1**, 114 (1989).
9. L. J. W. Shimon, M. Lahav, L. Leiserowitz, *J. Am. Chem. Soc.* **107**, 3375 (1985).
10. _____, *Nouv. J. Chim.* **10**, 723 (1986).
11. F. C. Wireko, L. J. W. Shimon, Z. Berkovitch-Yellin, M. Lahav. L. Leiserowitz, *J. Phys. Chem.* **91**, 471 (1987).
12. E. M. Landau *et al.*, *J. Am. Chem. Soc.* **111**, 1436 (1989); E. M. Landau *et al.*, *Pure Appl. Chem.* **61**, 673 (1989).
13. J. P. Legros and A. Kvick, *Acta Crystallogr. Sect. B* **36**, 3052 (1980).
14. I. Weissbuch *et al.*, *J. Am. Chem. Soc.* **105**, 6615 (1983).
15. Y. R. Shen, *The Principles of Nonlinear Optics* (Wiley, New York, 1984).
16. J. M. McBride and S. B. Bertman, *Angew. Chem. Int. Ed. Engl.* **28**, 330 (1989); *ibid.*, p. 377.
17. Z. Berkovitch-Yellin *et al.*, *J. Am. Chem. Soc.* **107**, 3111 (1985).
18. Y. Weissinger-Lewin *et al.*, *ibid.* **111**, 1035 (1989).
19. M. Vaida *et al.*, *ibid.*, p. 1029.
20. J. J. Verbist, M. S. Lehman, T. F. Koetzle, W. C. Hamilton, *Acta Crystallogr. Sect. B.* **28**, 3006 (1982).
21. M. Vaida *et al.*, *Science* **241**, 1475 (1988).
22. The original enunciation of Curie's principle [P. Curie, *J. Phys. (Paris)* (1894), p. 393] is as follows: "Lorsque certaines causes produisent certains effets, les éléments de symétrie des causes doivent se retrouver dans les effets produits. Lorsque certains effets révèlent une certaine dissymétrie, cette dissymétrie doit se retrouver dans les causes qui leur ont donné naissance. La réciproque de ces deux propositions n'est pas vrai, au moins pratiquement, c'est-a-dire que les effets produits peuvent être plus symétriques que les causes."
23. P. Bennema and G. Gilmer, in *Crystal Growth, an Introduction*, P. Hartman, Ed. (North-Holland, Amsterdam, 1973), pp. 263–327; M. Elwenspoek, P. Bennema, J. P. van der Eerden, *J. Cryst. Growth* **83**, 297 (1987).
24. J. R. Bourne and R. J. Davey, *ibid.* **36**, 278 (1976).
25. A. F. Wells, *Philos. Mag.* **37**, 184 (1946); *Discuss. Faraday Soc.* **5**, 197 (1949).
26. S. N. Black, R. J. Davey, T. D. McLean, *Mol. Cryst. Liq. Cryst. Inc. Nonlinear Opt.* **161**, 283 (1989).
27. L. J. W. Shimon, M. Vaida, L. Addadi, M. Lahav, L. Leiserowitz, *J. Am. Chem. Soc.* **112**, 6215 (1990).
28. L. J. W. Shimon *et al.*, *Mol. Cryst. Liq. Cryst* **137**, 67 (1986).
29. I. Weissbuch, D. Zbaida, L. Addadi, M. Lahav, L. Leiserowitz, *J. Am. Chem. Soc.* **109**, 1869 (1987).
30. D. Zbaida *et al.*, *React. Polym.* **6**, 241 (1987).
31. I. Weissbuch, L. Addadi, L. Leiserowitz, M. Lahav, *J. Am. Chem. Soc.* **110**, 561 (1988).
32. I. Weissbuch, F. Frolow, L. Addadi, M. Lahav, L. Leiserowitz, *ibid.* **112**, 7718 (1990).
33. S. Grayer Wolf *et al.*, *Nature* **328**, 63 (1987).
34. S. Grayer Wolf *et al.*, *Thin Solid Films* **159**, 29 (1988).
35. S. Grayer Wolf *et al.*, *Science* **242**, 1286 (1988).
36. D. Jacquemain *et al.*, *J. Am. Chem. Sox.* **112**, 7724 (1990).
37. M. Gavish, R. Popovitz-Biro, M. Lahav, L. Leiserowitz, *Science* **250**, 973 (1990).
38. D. Jacquemain *et al.*, *J. Am. Chem. Soc.*, in press.
39. F. Leveiller *et al.*, *Science*, in press.
40. E. M. Landau *et al.*, *Mol. Cryst. Liq. Cryst.* **134**, 323 (1986).
41. S. Mann, B. R. Heywood, S. Rajam, J. D. Birchall, *Nature* **334**, 692 (1988).
42. _____, *Proc. R. Soc. London Ser. A* **423**, 457 (1989).
43. H. A. Lowenstam and S. Weiner, *On Biomineralization* (Oxford Univ. Press, New York, 1989), chap. 3.
44. L. Addadi and S. Weiner, in *Biomineralization Chemical and Biochemical Perspectives*, S. Mann, J. Webb, R. J. P. Williams, Eds. (VCH, Weinheim, 1989), chap. 5.
45. A. Berman *et al.*, *Science* **250**, 664 (1990).

46. We thank L. J. W. Shimon, M. Vaida, and Y. L. Weissinger, who did the major share of the work described here as part of their Ph.D. theses, R. K. McMullan of the Brookhaven National Laboratory for his cooperation, E. Staab for his contribution as a Minerva postdoctoral fellow, and J. M. McBride for discussions. Supported by the United States–Israel Binational Science Foundation, Jerusalem, the Petroleum Research Fund, and the Minerva Foundation.